



HAL
open science

Dynamics of Vesicle Suspensions in Shear Flow Between Walls

Thomas Podgorski, Callens Natacha, Minetti Christophe, Gwennou Coupier,
Dubois Frank, Chaouqi Misbah

► **To cite this version:**

Thomas Podgorski, Callens Natacha, Minetti Christophe, Gwennou Coupier, Dubois Frank, et al.. Dynamics of Vesicle Suspensions in Shear Flow Between Walls. *Microgravity Science and Technology*, 2011, 23 (2), pp.263-270. 10.1007/s12217-010-9212-y . hal-00634494

HAL Id: hal-00634494

<https://hal.science/hal-00634494v1>

Submitted on 25 Oct 2011

HAL is a multi-disciplinary open access archive for the deposit and dissemination of scientific research documents, whether they are published or not. The documents may come from teaching and research institutions in France or abroad, or from public or private research centers.

L'archive ouverte pluridisciplinaire **HAL**, est destinée au dépôt et à la diffusion de documents scientifiques de niveau recherche, publiés ou non, émanant des établissements d'enseignement et de recherche français ou étrangers, des laboratoires publics ou privés.

Dynamics of vesicle suspensions in shear flow between walls

Thomas Podgorski · Natacha Callens ·
Christophe Minetti · Gwennou Coupier ·
Frank Dubois · Chaouqi Misbah

Received: date / Accepted: date

Abstract The behaviour of a vesicle suspension in a simple shear flow between plates (Couette flow) was investigated experimentally in parabolic flight and sounding rocket experiments by Digital Holographic Microscopy. The lift force which pushes deformable vesicles away from walls was quantitatively investigated and is found to be rather well described by a theoretical model by Olla [1]. At longer shearing times, vesicles reach a steady distribution about the center plane of the shear flow chamber, through a balance between the lift force and shear induced diffusion due to hydrodynamic interactions between vesicles. This steady distribution was investigated in the BIOMICS experiment in the MASER 11 sounding rocket. The results allow an estimation of self-diffusion coefficients in vesicle suspensions and reveal possible segregation phenomena in polydisperse suspensions.

Keywords Vesicle · Blood flow · Suspension · Lift force · Shear-induced diffusion

1 Introduction

Channel flows of complex fluids containing deformable particles such as red blood cells are influenced by many parameters such as deformability, hydrodynamic interactions between particles and between channel walls and particles. Qualitatively, several features of blood flow have been observed although their understanding is still incomplete:

T. Podgorski, G. Coupier, C. Misbah
Laboratoire de Spectrométrie Physique
CNRS - UJF Grenoble
140, rue de la Physique - BP 87
38402 Saint-Martin d'Hères Cedex, France
Tel.: +33-4-76514520
Fax: +33-4-76635495
E-mail: thomas.podgorski@ujf-grenoble.fr

N. Callens, C. Minetti, F. Dubois
Microgravity Research Center
Service de Chimie Physique CP 165/62
Université Libre de Bruxelles (ULB)
50 av. F. D. Roosevelt
1050 Bruxelles, Belgium

cell free layers near walls, different spatial distribution of RBCs (Red Blood Cells) and platelets, etc. These features play a decisive role in biological functions (cell adhesion and aggregation, immunitary response, rheology of blood in confined situations) and may be of interest in technological applications such as cell sorting devices, etc.

Over the years, giant lipid vesicles (closed lipid membranes of diameter between one and several hundred microns) have become a model for the study of deformable objects under flow. They reproduce the basic mechanical characteristics of RBCs (equilibrium shape, dynamics under flow [2]) while being simpler, more flexible and easier to manipulate: their geometrical and mechanical properties - size, deformability, viscosity - can be varied in a controlled fashion in order to get quantitative and predictive knowledge about their respective influence.

The ESA project BIOMICS (BIOMImetic and Cellular Systems) is dedicated to the study of vesicles suspensions under shear flow. The long term objectives of this study are a detailed understanding of the circulatory system and the rheology of deformable objects with potential new therapeutic means to prevent diseases.

The behaviour of vesicles under simple shear flow has been the subject of several theoretical and experimental studies (see [3] and references therein). When the viscosity ratio between the inner and outer fluids is small, vesicles follow a tank treading dynamics in which the orientation of the main axis of the vesicle is constant and the membrane undergoes a tank treading motion. When they are sheared close to a wall, a lift force of viscous origin appears which pushes vesicles away from the wall. This lift force is a consequence of the fore-aft asymmetry of the flow between the deformable vesicle and the wall : the pressure distribution due to the contraction and expansion of the flow is asymmetric (contrary to what would happen with a rigid sphere near a wall) and results in a net force [1,4,?].

As this lift force is easily screened by gravity forces, that cannot be completely removed if one wishes to control and vary other relevant parameters such as viscosity contrast, we studied it under microgravity conditions, by shearing vesicle suspensions between two plates. A first set of experiments were run in parabolic flight campaigns (ESA PF 43, CNES VP 59 and CNES VP 65), in order to determine the scaling of the lift velocity as a function of the relevant parameters (size R , distance to the wall z , deflation - or aspect ratio, and viscosity contrast λ).

Another important phenomenon in suspensions stems from the hydrodynamic interactions between particles. In suspensions of hard spheres, the interaction between two particles does not lead to any modification of the structure of the suspension because of the reversibility of the Stokes equation, and three-body interactions are necessary to break the symmetry of the problem. This is negligible in dilute suspensions. However in suspensions of deformable particles such as drops, vesicles or cells, the deformation of objects under shear breaks the fore-aft symmetry of the problem and a repulsion takes place between two particles when their trajectories meet under shear flow : the cross-streamwise distance between two objects is larger after they have met each other in the shear flow. This has been observed experimentally and numerically for drops and vesicles [5,6]. This repulsion between two vesicles is qualitatively similar to the repulsion between a vesicle and a wall mentioned above. The consequence at the scale of the suspension is a shear-induced self diffusion.

Therefore, when sheared between two plates, a vesicle suspension reaches a steady distribution where diffusion balances the migration of vesicles towards the center. As longer microgravity times are required to reach this steady state, a set of experiments was done in the Maser 11 sounding rocket and are presented here.

2 Experimental setup and procedures

2.1 Sample preparation

Vesicles were prepared by the electroformation method [7], from lipids (1,2 - Dioleoyl-sn-glycero-3-phosphocholine (DOPC)) deposited on ITO glass plates and an electroformation solution made of water, 20 % glycerol and 300 mM sucrose for sample 1 and water, 3.3 % dextran and 100 mM sucrose for sample 2. Each electroformation provides a polydisperse sample with vesicle diameters ranging from 5 to 100 μm (median size between 15 and 25 μm), a volume fraction of a few percent and a total volume of about 2 ml.

Samples were then diluted into a slightly hyperosmotic exterior solution made of water, glycerol and glucose (350 mM for sample 1 and 115 mM for sample 2), which leads to a partial deflation of vesicles, a difference of refractive index necessary for visualization in the digital holographic microscope, a density contrast responsible for sedimentation under gravity and a viscosity ratio η_{in}/η_{out} of 1.1 for sample 1 and 3.9 for sample 2. After dilution, the final volume fraction of vesicles was between 0.1 and 0.3 %.

2.2 Shear flow chamber

The experiments were performed in a Couette shear flow chamber designed and manufactured by the Swedish Space Corporation (SSC) for the MASER 11 sounding rocket. As shown on fig. 1, it is made of two parallel glass discs, with a diameter of 10 cm and a gap of 170 μm . The bottom disc is fixed and the top one can be rotated at constant speed by a computer controlled motor via a belt and a reducer, allowing shear rates between 0.5 and 50 s^{-1} . An inlet at the center of the bottom plate and several outlets at the periphery allow filling with experimental fluids, vesicle injection and rinsing. Vesicle suspensions and extra carrier fluid are contained in syringes connected to the inlet via flexible tubes. In parabolic flight experiments, a KDS syringe pump is used for the injections, and a soft pouch collects the excess and waste fluids. In the BIOMICS module of MASER 11, samples and rinsing fluid are contained in an injection unit made of Hamilton glass syringes and DC motors.

2.3 Digital Holographic Microscope

The observation system used to study the evolution and dynamics of the suspension is a digital holographic microscope (DHM) working with a partially coherent illumination designed and manufactured by the Microgravity Research Center (MRC) [8]. Digital holography allows to record rapidly the 3D information without scanning along the optical direction by changing the focus as with usual microscopy or confocal microscopy. The system uses a source of partial spatial coherence, created with a laser beam going through a rotating ground glass that reduces the amount of coherent artifact noise and the multiple reflection perturbations [9]. It is a Mach-Zehnder interferometer in microscope configuration. The shear flow chamber is placed in one arm of the interferometer in front of a microscope lens. The direction of observation is perpendicular to the plates, approximately 3 cm from the axis of rotation. The microscope lens, coupled

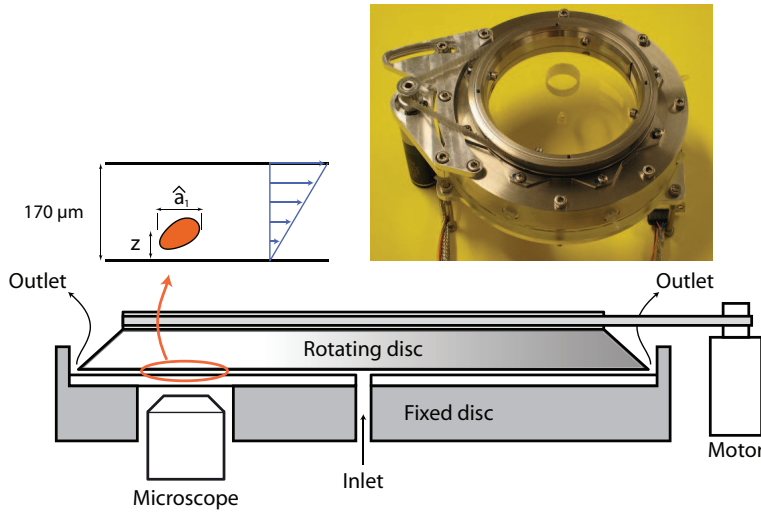


Fig. 1 Sketch and picture of the shear flow chamber.

with the refocusing lens, produces the image of one plane of the shear flow chamber thickness on the CCD. The second arm of the interferometer constitutes the reference beam and is also incident on the CCD where it is interfering with the object beam. The BIOMICS module developed by SSC for MASER 11, with its DHM (developed by Lambda-X) is depicted on fig. 2. In parabolic flights, a DHM built by MRC was used.

By recording the holographic data resulting from the interference pattern thanks to a CCD camera, the digital holographic microscope provides the capability to refocus numerically vesicles that are out of focus with respect to the focus plane of the optical imaging subsystem. The phase and intensity information are extracted from every hologram by the Fourier method [10,11] and the complex amplitude is computed and used to refocus it in any plane inside the shear flow chamber thickness [12]. The field of view of the digital holographic microscope is $(400 \mu\text{m})^3$. The image acquisition system is able to record 24 holograms/second. As the vesicles are transparent objects, when they are focused, it is necessary to take benefit of the phase information, to locate them in the experimental volume. Digital holographic reconstruction coupled to specific algorithmic techniques for object detection [12,13] permits to obtain the size, projected shape in the XY plane, 3D position, and an estimation of the mean velocity of each flowing vesicle.

3 Experimental study of the lift phenomenon

The lift undergone by vesicles when the suspension is sheared near a wall was investigated in parabolic flights. The case of vesicles with no viscosity contrast (Sample 1, $\lambda = 1.1$) was published in [3] and we summarize the main results here. Other viscosity contrasts were investigated recently during the PF50 ESA campaign and data are being processed.

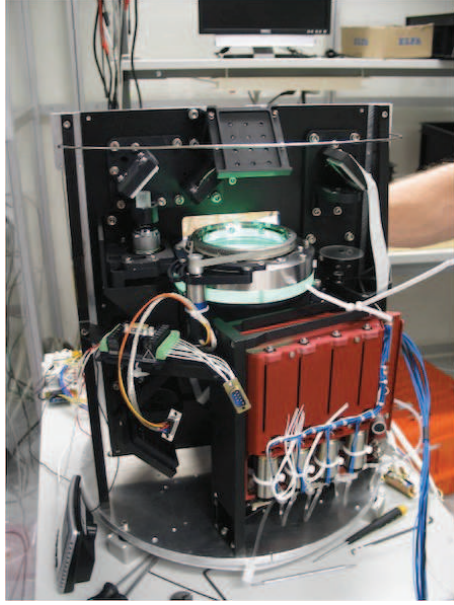


Fig. 2 BIOMICS module used in the MASER 11 flight. The green part is the shear flow chamber with its back illumination (for the overview camera), the red part is the injection device with its 4 syringes and motors, and the black breadboard is the DHM.

Parabolic flight in the A300-Zero G of Novespace consist in 31 parabolas, each providing 22 seconds of microgravity. Between parabolas (about 2.5 min), phases of normal and hyper gravity (1.5 to 1.8 g), during which the rotation of the shear flow chamber is stopped, allow a rapid sedimentation of the vesicles and provide a simple and reproducible initial condition with all vesicles lying on the bottom (fixed) disc. At the beginning of microgravity phases, the rotation of the chamber starts with shear rates between 0.5 and 50 s^{-1} and images are recorded at 24 holograms/s through the DHM while vesicles are lifted away from the bottom wall.

Between 5 and 20 vesicles with a diameter greater than 10 μm are detected on each image. We get the spatial distribution and shape of several thousand vesicles for each microgravity period. The z position (position in the migration direction) of the vesicles, as well as their (x, y) position in the plane parallel to the focal plane, are calculated. Each vesicle is characterized by its effective radius $\hat{R} = (\hat{a}_1 \hat{a}_2^2)^{1/3} / 2$ where \hat{a}_1 and \hat{a}_2 are the measured long and short axis of the projected vesicle shape and its aspect ratio \hat{a}_1 / \hat{a}_2 . Note that \hat{R} and \hat{a}_1 are apparent (projected) parameters (see fig. 1).

In the theoretical paper by Olla [1], it was proposed that the lift velocity of a vesicle scales as follow:

$$\frac{dz}{dt} = U(\lambda, \hat{a}_1 / \hat{a}_2) \dot{\gamma} \frac{R^3}{z^2}, \quad (1)$$

which gives by integration:

$$\left(\frac{z}{R}\right)^3 = 3U\dot{\gamma}t, \quad (2)$$

where R is the vesicle effective radius ($R = (a_1 a_2^2)^{1/3} / 2$ where a_1 and a_2 are the long and short axis of the vesicle shape), $\dot{\gamma}$ the shear rate, and z the distance to the wall.

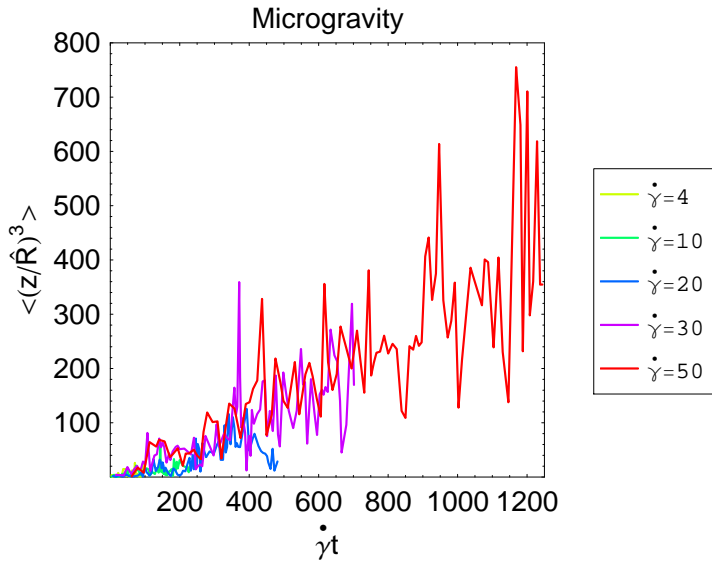


Fig. 3 Rescaled vesicle-wall distance $\langle (z^3/\hat{R}^3) \rangle$ vs $\dot{\gamma}t$ for different shear rates (filtering parameters: $5 < \hat{R} < 50 \mu\text{m}$, $1.1 < \hat{a}_1/a_2 < 1.25$; averaging over 15 detections).

This suggests to redraw the results with rescaled parameters $(z/\hat{R})^3 = (z/R)^3(a_1/\hat{a}_1)$ and $\dot{\gamma}t$. An example for one parabola is shown in fig. 3. Remarkably, all results fall on the same straight line, in agreement with eq. 2. The lift velocity decreases as the vesicle is moving far from the wall, but remains non-zero: hydrodynamic interactions are long range. Note that significant scattering is still present on this figure, partly due to statistics and mainly to vesicle dispersion linked to hydrodynamic interactions.

The slope of the data in fig. 3 is $\beta = 3U(a_1/\hat{a}_1)$, a function of vesicle aspect ratio and viscosity. The dependency of β upon vesicle aspect ratio a_1/a_2 is shown in fig. 4, and compared to Olla's prediction (with no fitting parameter). The agreement is quite satisfactory both qualitatively and quantitatively in the range of available aspect ratios, except above 1.2 where the number of corresponding vesicles decreases and statistics are not as favorable. The increase of lift velocity with the deflation is not systematic in general. For more viscous vesicles, a slow down in the migration upon deflation is predicted by Olla [1]. The data from PF50 ESA campaign should confirm this trend, that we already observed in the case of migration in a channel (Poiseuille flow) [14].

For an isolated vesicle, the lift forces exerted by the two walls of the shear chamber will eventually lead to a steady state where the vesicle will be exactly in the middle of the chamber. In a many vesicles configuration, interactions between them will modify this steady state and lead to a wider distribution in the chamber. In parabolic flight experiments, this state cannot be reached due to too short microgravity period, but this was made possible by installing the experiment in a sounding rocket.

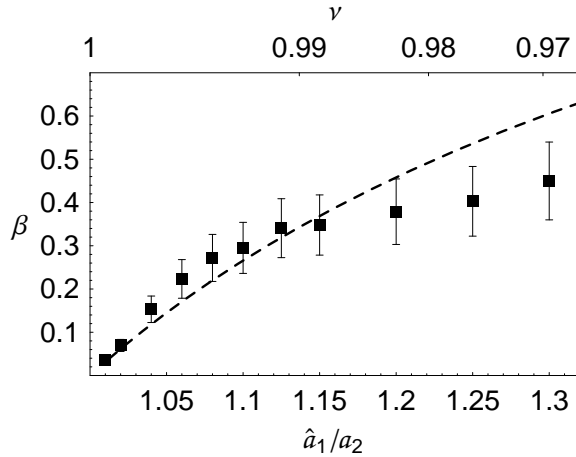


Fig. 4 Lift parameter β vs vesicle aspect ratio \hat{a}_1/a_2 determined from experimental data. Top horizontal axis: corresponding values of the reduced volume $\nu = 3V(4\pi)^{1/2}/S^{3/2}$ where V and S are the vesicle's volume and surface area. Dashed line: theoretical prediction from Olla [1].

4 Equilibrium distribution of the suspension

In the MASER 11 flight, the two samples 1 and 2 were studied, with viscosity ratios of 1.1 and 3.9. During the 5 minutes and 49 s of microgravity, after filling the chamber with rinsing fluid (without vesicles), samples were injected before each shearing sequence. Sample 1 was sheared with a shear rate of $\dot{\gamma} = 50 \text{ s}^{-1}$ for 25 s, then $\dot{\gamma} = 12.5 \text{ s}^{-1}$ for 25 s without re-injecting, then $\dot{\gamma} = 25 \text{ s}^{-1}$ for 50 s and $\dot{\gamma} = 12.5 \text{ s}^{-1}$ for 100 s after new injections. Sample 2 was sheared at $\dot{\gamma} = 50 \text{ s}^{-1}$ for 25 s, and, then $\dot{\gamma} = 25 \text{ s}^{-1}$ for 50 s.

Contrary to parabolic flights, injection was made in microgravity and no sedimentation took place. Therefore the suspension was initially centered in the flow chamber. In addition, because of the distance between the injection point (center of the chamber) and the observation point (about 34 mm from the center), some migration of vesicles took place during the injection. Thanks to the good quality of images and samples, a large number of vesicles was detected (between 500 and 1000 per second at 25 fps).

An example of vesicle distribution is shown in fig. 5. From this raw data, one can extract the density profile of vesicles across the thickness (number of vesicles per unit volume vs. distance from bottom wall) presented in the following figures. As seen on this figure, the width of the distribution decreases slowly with time, as vesicles gather at the center of the flow chamber and a steady distribution is reached under the balance between lift forces from both walls and shear induced diffusion.

A strong influence of vesicle size was observed (see fig. 6) : for a given range of vesicle aspect ratio (or reduced volume), large vesicles are much more concentrated around the center plane of the flow chamber than smaller vesicles. A similar influence of the vesicle shape is observed: deflated vesicles are more centered than nearly spherical ones. This can be quantitatively seen in fig. 7.

While it is known from studies on the lift phenomenon presented in the previous section that the lift force increases with vesicle size and deflation, the influence of these parameters on shear induced diffusion coefficients is still unclear at this point.

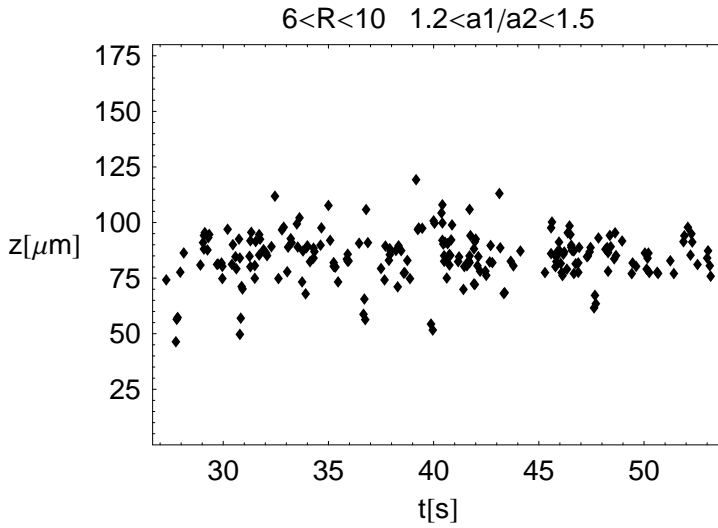


Fig. 5 Detected vesicles in the range of size $6 > R > 10 \mu\text{m}$ and of aspect ratio $1.2 < a_1/a_2 < 1.5$, for sample 1 at a shear rate of $\dot{\gamma} = 50 \text{ s}^{-1}$.

In order to extract quantitative information from this data, a simple modelling attempt is based on a balance between a convective flux due to lift forces and a diffusive flux due to shear induced diffusion, which, at equilibrium, should give rise to a steady distribution of vesicles in the chamber's thickness.

Following the good agreement of Olla's prediction with the results from parabolic flights for the lift due to the presence of one wall, we assume that the lift velocity due to the presence of two walls at $z = 0$ and $z = h$ can be computed by a linear superposition of the contributions of each wall. As the flow is completely anti-symmetric with respect to the midplane $z = h/2$, we get:

$$u(z) = U(\lambda, \nu) \dot{\gamma} R^3 \left(\frac{1}{z^2} - \frac{1}{(h-z)^2} \right) \quad (3)$$

The corresponding flux of vesicles is thus:

$$J_C = n(z)u(z) \quad (4)$$

There has been, to date, no systematic study, either experimental, numerical or theoretical study investigating pairwise interactions between vesicles, although a paper by Kantsler and Steinberg [5] shows a few examples of interactions and vesicle trajectories. Loewenberg and Hinch [6] made a numerical study of shear induced diffusion in an emulsion of droplets. Although drops and vesicles have different mechanical properties, we assume here that the same scaling holds for the diffusivity of vesicles:

$$D = f_2 \Phi \dot{\gamma} R^2 = \frac{4\pi}{3} f_2 n(z) \dot{\gamma} R^5 \quad (5)$$

where Φ is the volume fraction of vesicles, R their radius, $n(z)$ the local concentration of vesicles (number per unit volume) and f_2 a dimensionless diffusion constant (of order 0.1 for drops).

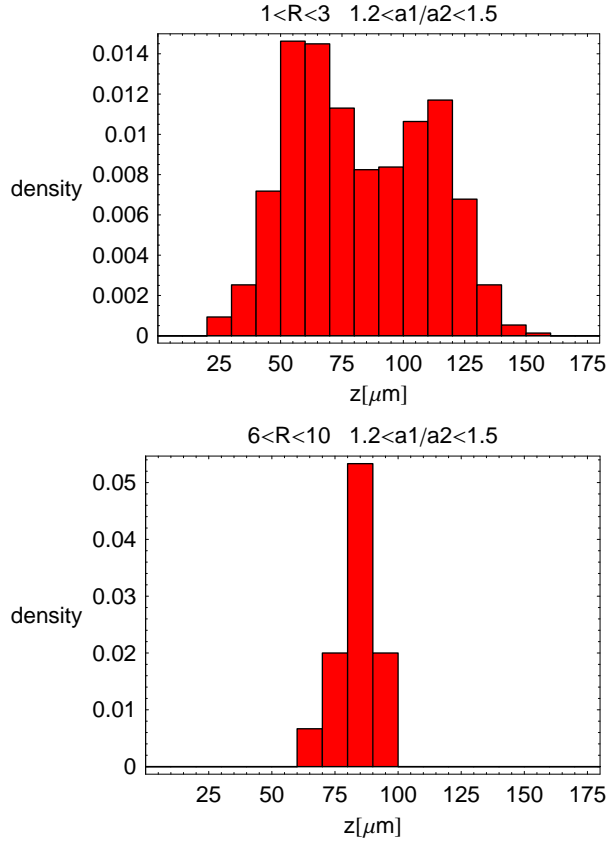


Fig. 6 Comparison of the final distributions of small (top) and large (bottom) vesicles for the same range of aspect ratio a_1/a_2 .

The corresponding diffusive flux is then:

$$J_D = -D \frac{\partial n}{\partial z} \quad (6)$$

The steady distribution, for a monodisperse suspension, is obtained for a zero total flux $J_C + J_D = 0$:

$$n(z) = \frac{n_{max}}{2w^2} \left(h^2 + w^2 - \frac{h^2(h^2 - w^2)}{4z(h-z)} \right) \quad (7)$$

The shape of this model distribution is shown in fig. 8.

From the parameters of this distribution (width w and height n_{max}) which can be measured from MASER 11 experiments, and the amplitude of the lift velocity U assumed to be given by Olla's theory, one can extract experimental diffusion coefficients with the following relation:

$$f_2 = \frac{6Uw^2}{\pi R^2 n_{max} h(h^2 - w^2)} \quad (8)$$

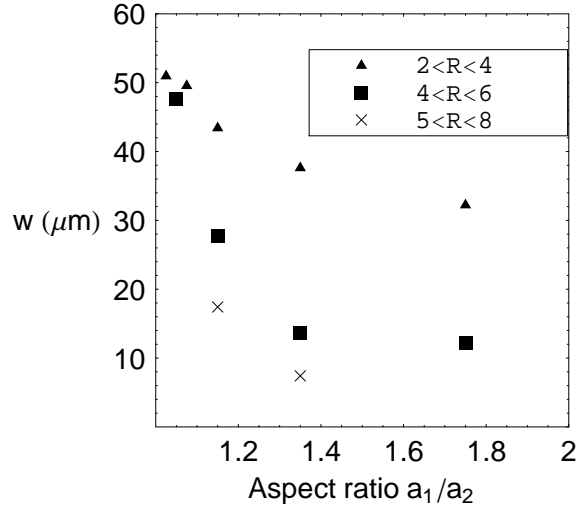


Fig. 7 Width of the vesicle distribution vs. aspect ratio a_1/a_2 .

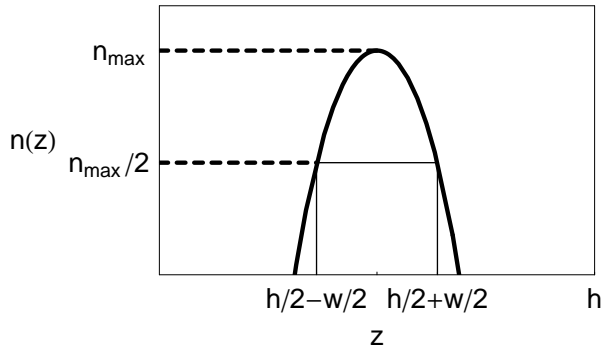


Fig. 8 Concentration profile of vesicles as predicted by eq. 7.

Note that this model only strictly holds for monodisperse samples where a single diffusion coefficient can be defined. Therefore we can only measure effective diffusion coefficients in a polydisperse sample from experimental distributions using this model. Some results are shown in fig. 9. For the largest vesicles the measured diffusion coefficient is of order 0.1, which is the same order of magnitude as observed for monodisperse droplet suspensions [6]. This means that large vesicles in a polydisperse suspension behave nearly as if they were alone and are weakly influenced by the presence of smaller vesicles. On the other hand, for small vesicles, the diffusion coefficient is orders of magnitude higher, suggesting a strong repulsion by bigger vesicles.

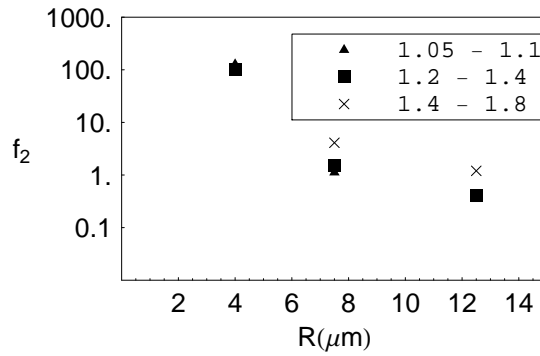


Fig. 9 Experimental measurements of the diffusion constant f_2 vs. vesicle size.

This last result suggests that segregation effects can take place in a polydisperse sample, where small vesicles should be pushed out of the center zone by bigger ones, as observed in blood microcirculation where small platelets seem to be closer to vessel walls than bigger red blood cells.

5 Conclusions and perspectives

We have studied the lift force undergone by a vesicle suspension under shear flow near a wall in parabolic flights as well as its equilibrium distribution after longer microgravity times in MASER 11. PF experiments on samples with a viscosity ratio close to 1 revealed that the lift dynamics was well described by Olla's theory, while MASER 11 results allowed the first measurements of a diffusion constant in vesicle suspensions. The strong dependence of steady distributions on vesicle properties is responsible for segregation effects which are potentially important in biological flows and could be used in applications such as cell-sorting.

These investigations are currently being extended by systematically studying the influence of the viscosity contrast on the lift force (ESA PF 50 and 51). A precise determination of self-diffusion coefficients requires to work with monodisperse samples, as well as bidisperse samples in order to measure inter-species diffusion coefficients. A method for producing such samples has been tested and experiments parabolic flights (ESA PF 51) and sounding rockets (MASER 12) are planned. In parallel, a systematic study of hydrodynamic interactions at the microscopic scale will be done.

Acknowledgements The authors wish to thank ESA and CNES for access to sounding rocket and parabolic flights and financial support. This work was supported by the SSTC/ESA-PRODEX contract 90171. The shear flow chamber used for parabolic flights was kindly provided by the Swedish Space Corporation (SSC). We thank V. Vitkova for experimental advice and help, C. Lockowandt (SSC) for assistance, J. Giraud, P. Ballet and A. Muylaert for experimental design and technical assistance. GC acknowledges support by a CNES postdoctoral fellowship.

References

1. Olla P., The lift on a tank-treading ellipsoidal cell in a shear flow, *J. Phys. II France*, 7, 1533 (1997)
2. Vitkova V., Mader M.-A., Polack P., Misbah C. Podgorski T., Micro-macro link in rheology of erythrocyte and vesicle suspensions, *Biophys. J.* 95, 33 (2008)
3. Callens N., Minetti C. Coupier G., Mader M.-A., Dubois F., Misbah C. Podgorski T., Hydrodynamical lift of vesicles under shear flow in microgravity, *Europhys. Lett.* 83, 24002 (2008)
4. Cantat I. Misbah C., Lift force and dynamical unbinding of adhering vesicles under shear flow, *Phys. Rev. Lett.* 83, 880 (1999)
5. Kantsler V., Segre E. Steinberg V., Dynamics of interacting vesicles and rheology of vesicle suspension in shear flow, *Europhys. Lett.* 82, 58005 (2008)
6. Loewenberg M. Hinch E. J., Collision of two deformable drops in shear flow, *J. Fluid Mech.* 338, 299 (1997)
7. Angelova M.L., Soleau S., Meleard P., Faucon J.-F. Bothorel P., Preparation of giant vesicles by external A.C. electric fields. Kinetics and applications, *Prog. Colloid Polym. Sci.* 89, 127 (1992)
8. Dubois F., Callens N., Yourassowsky C., Hoyos M., Kurowski P. Monnom O., Digital Holographic Microscopy with reduced spatial coherence for 3-dimensional particle flow analysis, *Appl. Opt.* 45, 864 (2006)
9. Dubois F., Novella Requena M.-L., Minetti C., Monnom O. Istasse E., Partial coherence effects in digital Holographic Microscopy with a laser source, *Appl. Opt.* 43, 1131 (2004)
10. Takeda M., Ina H. Kobayashi S., Fourier transform method of fringe pattern analysis for computer based tomography and interferometry, *J. Opt. Soc. Am.* 72, 156 (1982)
11. Kreis T., Digital Holographic interference phase measurements using the Fourier transform method, *J. Opt. Soc. Am. A* 3, 847 (1986)
12. Dubois F., Schockaert C., Callens N. Yourassowsky C., Focus Plane detection criteria in Digital Holographic Microscopy by amplitude analysis, *Optics Express* 14, 5895 (2006)
13. Dubois F., Monnom O., Yourassowsky C. Legros J.-C., Border processing in Digital Holography by extension of the digital hologram and reduction of the higher spatial frequencies, *Appl. Opt.* 41, 2621 (2002)
14. Coupier G., Kaoui B., Podgorski T. Misbah C., Noninertial lateral migration of vesicles in bounded Poiseuille flow, *Phys Fluids* 20, 11702 (2008)